https://doi.org/10.5194/acp-2021-461
Preprint. Discussion started: 17 June 2021
© Author(s) 2021. CC BY 4.0 License.

Atmospheric Chemistry and Physics Discussions
Open Access

# Eastward-propagating planetary wave in the polar middle atmosphere

Liang Tang[1], Sheng-Yang Gu[1*], Xian-Kang Dou[1]

[1] Electronic Information School, Wuhan University, Wuhan, China.

*Corresponding author: Sheng-Yang Gu, (gushengyang@whu.edu.cn)

https://doi.org/10.5194/acp-2021-461
Preprint. Discussion started: 17 June 2021
© Author(s) 2021. CC BY 4.0 License.



**Abstract.** We presented the global variations of the eastward propagating wavenumber 1 (E1), 2 (E2), 3 (E3), and 4 (E4) planetary waves (PWs) and their diagnostic results in the polar middle atmosphere, using MERRA-2 temperature and wind datasets in 2019. It is clearly shown that the eastward wave modes exist during winter periods with westward background wind in both hemispheres. The maximum wave amplitudes in the southern hemisphere (SH) are slightly larger and lie lower than those in the northern hemisphere (NH). It is also found that the wave perturbations peak at lower latitudes with smaller amplitude as the wavenumber increases. The period of the E1 mode varies from 3 to 5 days in both hemispheres, while the period of E2 mode is slightly longer in the NH (48 h) than in the SH (40 h). The periods of the E3 are ~30 h in both SH and NH, and the period of E4 is ~24 h. Though the wave periods become shorter as the wavenumber increases, their mean phase speeds are relatively stable, which are ~53, ~58, ~55, and ~52 m/s at 70° latitudes for W1, W2, W3, and W4, respectively. The eastward PWs occur earlier with increasing zonal wavenumber, which agrees well with the seasonal variations of the background zonal wind through the generation of critical layers. Diagnostic analysis also shows that the mean flow instability in the upper stratosphere and upper mesosphere may both contribute to the amplification of the eastward PWs.

https://doi.org/10.5194/acp-2021-461
Preprint. Discussion started: 17 June 2021
© Author(s) 2021. CC BY 4.0 License.

Atmospheric Chemistry and Physics Discussions

## 1 Introduction

Large amplitude planetary waves are dominant in the stratosphere, mesosphere, and lower thermosphere region and their interaction with zonal mean winds is the primary driving force of atmospheric dynamics. In addition, sudden stratospheric warmings (SSWs) and quasi-biennial oscillation (QBO) events can dynamically couple the entire atmosphere from the lower atmosphere to the ionosphere (Li et al., 2020; Yamazaki et al., 2020; Yadav et al., 2019; Matthias and Ern, 2018; Stray et al., 2015). Westward propagating planetary wave is one of the prominent features during austral and boreal summer periods. Westward quasi-2-day waves (Q2DWs) are the most obvious representative waves and one of the most investigated phenomena by planetary wave observations. Most previous studies focused on westward propagating Q2DWs, including zonal wavenumbers of 2 (W2), 3 (W3), and 4 (W4) modes (Lainer et al., 2018; Gu et al., 2018c; Wang et al., 2017; Pancheva et al., 2017; Gu et al., 2016a; Gu et al., 2016b; Lilienthal and Jacobi, 2015; Gu et al., 2013; Limpasuvan and Wu, 2009; Salby, 1981). The seasonal variations of the occurrence date, peak amplitude, and wave period for eastward Q2DWs are rarely studied (Gu et al., 2017; Lu et al., 2013; Alexander and Shepherd, 2010; Venne and Stanford, 2010; Merzlyakov and Pancheva, 2007; Palo et al., 2007; Sandford et al., 2007; Manney et al., 1993).

Q2DWs usually maximize after the summer solstice in middle

https://doi.org/10.5194/acp-2021-461
Preprint. Discussion started: 17 June 2021
© Author(s) 2021. CC BY 4.0 License.



latitudes. The largest wave amplitudes are observed near the mesopause in January–February in the Southern Hemisphere (SH), while in the Northern Hemisphere (NH) in July–August (Tunbridge et al., 2011). The W3 and W4 Q2DWs reach a maximum amplitude during austral and boreal summer periods in the mesosphere and lower thermosphere, respectively. The westward Q2DWs activity has an obvious seasonal variation (Liu et al., 2019; Gu et al., 2018d; Rao et al., 2016). Tunbridge et al. (2011) have long-term observed Q2DW in the NH and SH, and found that the W3 is generally stronger than those of the other two modes in the SH, reaching an amplitude of 12 K, while the W4 is stronger than W3 in the NH and can reach 4 K. W4 is generally longer lived than W3, and W4 is still observed after W3 has ended. The results of Liu and H.-L. (2004) show that the wave source, instability, critical layer and mean zonal wind structure are the primary reasons for the seasonal variation of Q2DWs. Gu et al. (2018d) have the long-term observation of satellite datasets in the SH and found that the strongest events of W2, W3, and W4 are delayed with increasing the zonal wavenumber and would be confused during the SSWs period. Then the wave period of W3 primarily fluctuated in 45-52 h, while the W4 varies is concentrated between 41-56 h, and the W2 is primarily distributed in 45-48 h. In addition, W2 can be observed in global satellite datasets, showing weaker amplitude in the NH and SH (Meek et al., 1996). The propagation and amplification of Q2DWs are primarily dominated by

https://doi.org/10.5194/acp-2021-461
Preprint. Discussion started: 17 June 2021
© Author(s) 2021. CC BY 4.0 License.


instability, refractive index, and critical layer, while the variation of background wind may cause different zonal wavenumber events (Gu et al., 2016a; Gu et al., 2016b). Xiong et al. (2018) studied variations in Q2DWs activity during the SSWs period and found that W1 was generated by the nonlinear interaction between SPW2 and W3. Gu et al. (2018c) found that the coupling between the NH and SH enhanced the summer easterly during SSWs and promoted the nonlinear interaction between W3 and SPW1 during the SSWs period.

Recent studies have found significant eastward planetary waves activity in the polar stratosphere and mesosphere regions, with near 2 and 4 days in the wave periods (Gu et al., 2017; Venne and Stanford, 2010; Merzlyakov and Pancheva, 2007; Sandford et al., 2007; Coy et al., 2003; Manney et al., 1993). Planetary waves with zonal wavenumbers -1 (E1) and -2 (E2) correspond to 4- and 2-day waves, respectively. In addition, the planetary waves of 1.2-day with wavenumber -3 (E3) and 0.8-day with wavenumber -4 (E4) have been found same phase speeds as the 2- and 4-day waves (Manney et al., 1993). This series of eastward propagating planetary waves have a significant effect on the thermal and dynamic structure of the polar stratosphere, resulting in significant wind and temperature variations in the polar stratosphere (Venne and Stanford, 2010; Coy et al., 2003). Palo et al. (1999) demonstrated a series of nonlinear interactions between the migrating tides and Q2DWs. Further research,

https://doi.org/10.5194/acp-2021-461
Preprint. Discussion started: 17 June 2021
© Author(s) 2021. CC BY 4.0 License.
Atmospheric Chemistry and Physics Discussions

Palo et al. (2007) presented evidence that the eastward Q2DW was coupled by the nonlinear planetary wave and the tides in the mesosphere and lower thermosphere.

Merzlyakov & Pancheva. (2007) analyzed and studied satellite datasets and they observed the eastward propagating wave with the zonal wave numbers -1 and -2 in February 2004, while E1 and E2 events with wave periods within 1.5-5 days. They found that the direction of EP fluxes for eastward planetary waves is from the upper layer to the lower atmosphere, suggesting that the upper atmosphere has a dynamic influence on the lower atmosphere. Sandford et al. (2007) reported a significant Q2DW fluctuation in the polar mesosphere with a zonal wavenumber of -2 (E2). They found that variations of mean zonal wind during a major SSW period can affect the propagation of polar E2. In addition, they believe that E2 fluctuation is representative in the mesosphere and caused by the instabilities in the polar night jet. Gu et al. (2017) proposed that the amplitude of E2 can reach 10K, 20 m/s, and 30 m/s in temperature, zonal wind, and meridional wind in the austral winter period, while the amplitude of E2 decreases by near two-thirds in the boreal winter period. Lu et al. (2013) found that the propagation height of eastward planetary waves was limited to the winter high latitudes, which may be caused by the negative refractive index of 45°S at the equator, thus preventing the planetary wave propagation to the low latitudes. They believe that the instability region at

50-60°S may be induced by the stratospheric polar night jet and/or the "double-jet" structure.

The second modern retrospective research and application analysis (MERRA-2) datasets are used to investigate the eastward propagation wave characteristics during 2019 in the polar stratospheric and mesospheric region, including zonal wavenumbers -1 (E1), -2 (E2), -3 (E3) and -4 (E4). Particularly, our study is to explore the variation of occurrence date, peak amplitude, and wave period for eastward wave and the role of instability, background wind structure, and critical layer for the eastward wave propagation and amplification. The remaining parts of this paper are organized as follows. Section 2, the data and methods used in our study are described. Section 3 analyzes the global latitude-temporal variation structure of eastward waves in the winter of 2019. The amplification and propagation features of different wavenumber events for eastward planetary waves in the NH and SH are investigated in Section 3.1 and 3.2, respectively. Section 3.3 will compare and analyze eastward waves in the NH and SH. Section 4 summarizes our research results.

## 2 Data and Analysis

The least-square method is applied to each time window to extract the E1-, E2-, E3-, and E4-wave, with 10-day, 6-day, 4-day, and 4-day, and is used by us to determine the amplitude (Gu et al., 2013). This method has previously been used successfully to identify planetary waves from

https://doi.org/10.5194/acp-2021-461
Preprint. Discussion started: 17 June 2021
© Author(s) 2021. CC BY 4.0 License.
Atmospheric Chemistry and Physics Discussions
Open Access
EGU

satellite measurements (Gu et al., 2018a; Gu et al., 2018b; Gu et al., 2018c; Gu et al., 2018d).

$$y = A\cos[2\pi(\sigma \cdot t + s \cdot \lambda)] + B\sin[2\pi(\sigma \cdot t + s \cdot \lambda)] + C \quad (1)$$

The least-squares method is used to fit the parameters of ( $A$, $B$ and $C$ ). Where ( $\sigma, t, s$ and $\lambda$ ) are the frequency, zonal wavenumber, UT time, and longitudes. The amplitude $R$ of wavenumber could be expressed as $R^2 = \sqrt{A^2 + B^2}$ .

The second modern retrospective research and application analysis (MERRA-2) data is a set of long-term atmospheric reanalysis datasets started by NASA in 1980, and now using an upgraded version of the Goddard Earth Observing System Model, Version 5 (GEOS-5) data assimilation system. MERRA-2 includes updates to the model (Molod et al., 2015; Molod et al., 2012) and the Global Statistical Interpolation (GSI) analysis scheme of Wu et al. (2002). The MERRA-2 data includes various meteorological variables such as net radiation, temperature, relative humidity, wind speed, etc. The MERRA-2 data covers the world, with a spatial resolution of 0.5°*0.625° and a temporal resolution of 1 hour. This kind of meteorological data is widely used to detect the middle atmosphere such as the planetary wave in the polar atmosphere, global thermal tides, climate variability, and aerosol (Sun et al., 2020; Ukhov et al., 2020; Bali et al., 2019; Lu et al., 2013). These studies indicate that MERRA-2 data can be used in our research with high authenticity. The MERRA-2 datasets

https://doi.org/10.5194/acp-2021-461
Preprint. Discussion started: 17 June 2021
© Author(s) 2021. CC BY 4.0 License.

Atmospheric Chemistry and Physics Discussions

are used to obtain the variation in background wind, instability, refractive index, and critical layer, and explore the rules of eastward planetary waves propagation and amplification through diagnostic analysis.

The critical layer will absorb or reflect planetary waves during upward propagation from the lower atmosphere. The planetary wave will be amplified from the reflection process after gaining sufficient energy in the instability region. This shows that the critical layer plays an important role in regulating the amplification and propagation of planetary waves (Gu et al., 2016a; Gu et al., 2016b; Liu and H.-L., 2004). The baroclinic/barotropic instability in the atmospheric space structure is caused by the simultaneous equalization of the negative latitude gradient and the quasi-geostrophic potential vorticity ($\overline{q_\varphi}$). Where ($\Omega$) denote the angular speed of the Earth's rotation, and the latitude and zonal mean zonal wind are represented by ($\varphi$ and $\bar{u}$), in the second part, the ($a$) represents the Earth radius, in the last part, ($\rho$, $f$, and $N$) denote the background air density, Coriolis parameter, and buoyancy frequency, respectively. The vertical and latitudinal gradients are represented by subscripts ($z$ and $\varphi$).

$$\overline{q_\varphi} = 2\Omega\cos\varphi - \left(\frac{\left(\bar{u}\cos\varphi\right)_\varphi}{a\cos\varphi}\right)_\varphi - \frac{a}{\rho}\left(\frac{f^2}{N^2}\rho\bar{u}_z\right)_z \qquad (2)$$

Andrews et al. (1987) define the Eliassen-Palm (EP) flux vectors (F) to show the properties of planetary wave propagation, calculated as follows:

https://doi.org/10.5194/acp-2021-461
Preprint. Discussion started: 17 June 2021
© Author(s) 2021. CC BY 4.0 License.


$$F = \rho a \cos\varphi \begin{bmatrix} \dfrac{\overline{u}_z \overline{v'\theta'}}{\overline{\theta}_z} - \overline{v'u'} \\ \left[ f - \dfrac{\left(\overline{u}\cos\varphi\right)_\varphi}{a\cos\varphi} \right] \dfrac{\overline{v'\theta'}}{\overline{\theta}_z} - \overline{w'u'} \end{bmatrix} \quad (3)$$

Where $u'$ and $v'$ are the planetary wave perturbations in the zonal and meridional wind, $\theta'$ and $w'$ represent potential temperature and vertical wind, respectively. The planetary wave propagation is only favorable where the square of refractive index $m^2$ was positive:

$$m^2 = \frac{\overline{q}_\varphi}{a\left(\overline{u} - c\right)} - \frac{s^2}{\left(a\cos\varphi\right)^2} - \frac{f^2}{4N^2H^2} \quad (4)$$

Where ( $s$ ) denote the zonal wavenumber, the phase speed is represented by ( $c$ ), and the ( $H$ ) represents the scale height. The square of the refractive index is taken as the waveguide of planetary waves.

## 3 Results and Discussion

The global temporal-latitude variation structures of E1, E2, E3, and E4 extracted from the 2019 MERRA-2 temperature datasets using time windows of 10-, 6-, 4- and 4-days respectively are shown in Figure 1. The mean temperature amplitudes of E1, E2, E3, and E4 at 55.4km during periods of 3~5-, 1.5~2.5-, 1~1.5-, and 0.9~1.1-days are shown in Figure1a, 1b, 1c, and 1d. The eastward wave modes during winter periods in the SH and NH are characterized by obvious seasonal variations. In addition, the E1, E2 (E3), and E4 reach the maximum amplitudes at 50-80°(S/N). In the SH, the strongest events of E1 and E2 occur on days 209-218 and 167-172, while those of E3 and E4 occur on 151-154 and 139-142 days. This shows

https://doi.org/10.5194/acp-2021-461
Preprint. Discussion started: 17 June 2021
© Author(s) 2021. CC BY 4.0 License.



that the occurrence date of maximum amplitude occurs earlier with increasing zonal wavenumber. In addition, the maximum amplitudes of E1, E2, E3, and E4 are 6.0K, 4.2K, 3.6K, and 2.4K, indicating that the peak amplitudes decrease with increasing zonal wavenumber. In the NH, the occurrence dates of the strongest events of E1, E2, E3, and E4 are days 41-50, 69-74, 35-38, and 63-66, and the corresponding peak amplitudes are 5.5K, 3.8K, 2.8K, and 1.2K. It is found that the peak amplitude also decreases with increasing zonal wavenumber in the NH, but their occurrence dates vary irregularly. In addition, the E4 is weak in the NH and almost impossible to find, so W4 is out of the discussion in the NH. Figure 2 shows that the 2019 zonal mean zonal wind variations at 70˚S and 70˚N. It is clearly shown that the eastward wave modes exist during winter periods with westward background wind in both hemispheres.

### 3.1 In the Southern Hemisphere

Figure 3 shows that the E1, E2 (E3), and E4 are distributed in ~70-80˚S, ~60-70˚S, and ~50-60˚S at ~48.2km, respectively. E1 events occur on days 161-170, 187-196, 211-220, and 231-240, respectively, and the maximum fluctuation on days 211-220 is ~8.5K, as shown in Figure 3a. In addition, the wave period of E1 decreased from the maximum ~106 h (days 187-196) to ~69 h (days 211-220), indicating the instability of the E1 wave period. E2 events occur on days 139-144, 173-178, 187-192, and 219-224, and the maximum amplitude of ~7.8K occurs on days 219-224, and the

https://doi.org/10.5194/acp-2021-461
Preprint. Discussion started: 17 June 2021
© Author(s) 2021. CC BY 4.0 License.


wave period of E2 is stable approximate 40 h (Figure 3b). The strongest E3 event occurs on days 151-154, and the rest are distributed on days 141-144, 201-204, 209-202, and shows E3 wave period approximate 29 h, as shown in Figure 3c. From Figure 3d, E4 events are distributed on days 127-130, 145-148, 161-164, 213-216, with a weak amplitude of about ~3K, while the wave period is stable at near 24 h. In addition, we found that the planetary waves E1, E2, E3, and E4 have similar phase speeds.

The spectra, spatial structures of temperature, zonal and meridional wind, and diagnostic analysis of E1 are extracted from the corresponding two representative events, as shown in Figure 4. The E1 planetary wave has a wave period of ~106 h and ~69 h on days 187-196 and 211-220 (Figures 4a and 4b). The temperature spatial structure of E1 events presents an obvious dual structure of amplitudes at ~50km and ~60km, as displayed in Figures 4c and 4d. The strongest temperature amplitude of E1 occurs at ~50 km and ~70-80˚S with an amplitude of ~10K on the days 211-220, and the other peak is ~9K (60km). The temperature amplitude of ~9K occurs on days 187-196, and the rest is ~7K (60km). The spatial structures of zonal wind and meridional wind of E1 are shown in Figures 4e, 4f, 4g, and 4h. The maximum amplitudes of zonal and meridional winds occur at ~60˚S and ~60km, and ~80˚S and ~60km. The amplitude of zonal and meridional wind reaches ~14 m/s and ~20 m/s, and ~10m/s and ~17m/s on days 187-196 and 211-220, respectively. From Figure 4i, E1 EP flux presents two

https://doi.org/10.5194/acp-2021-461
Preprint. Discussion started: 17 June 2021
© Author(s) 2021. CC BY 4.0 License.



directions of propagation. It is clear that the E1 is more favorable to propagate in the winter hemisphere and is dramatically amplified by the mean flow instabilities and appropriate background winds at polar and middle latitudes between ~40 and ~80 km, where the former propagate to the upper atmosphere and the latter to the lower atmosphere. In addition, E1 is amplified by wave-mean flow interactions near its critical layer (106 h). The strong instability and weak background wind and positive refractive index region provide sufficient energy for the upward EP flux to propagate and amplify. However, the downward EP flux is propagated and amplified by the interaction of the critical layer in the positive refractive index region, where the strong background wind and weak instability provide sufficient energy. In addition, both upward and downward EP fluxes eventually propagate toward the equator at ~50km. Figure 4j shows that EP flux propagates downward and amplifies after the interaction of the critical layer (~69 h), which strong instability and strong background wind provide energy, and ultimately point towards the equator. We believe that the weak background wind and strong instability in the polar region promote the upward propagation and amplification of the EP flux. In addition, the strong background wind and weak instability in the middle latitudes are not conducive to the downward propagation and amplification of the EP flux. In other words, instability and appropriate background wind play a dominant role in the propagation and amplification of the E1.

https://doi.org/10.5194/acp-2021-461
Preprint. Discussion started: 17 June 2021
© Author(s) 2021. CC BY 4.0 License.


From Figures 5a and 5b, the wave periods of E2 planetary waves are 38 h and 39 h on days 173-178 and 219-224. The temperature spatial structure of E2 events shows an obvious amplitude dual structure (Figures 5c and 5d). The maximum temperature amplitude of the E2 event on days 219-224 and 173-178 is ~9K (~50km) and ~7K (~50km). The spatial structures of zonal wind and meridional wind of E2 are shown in Figures 5e, 5f, 5g, and 5h. The maximum amplitudes of zonal and meridional winds occur at ~60˚S and ~60km, and ~80˚S and ~60km. The maximum amplitude of zonal wind reaches ~10 m/s and ~20 m/s, while the meridional wind is slightly stronger than the zonal wind, which reaches ~13 m/s and ~27 m/s on days 173-178 and 219-224. From Figures 5i and 5j, it is clear that the E2 is more favorable to propagate in the SH winter and is dramatically amplified by the mean flow instabilities at middle-high latitudes between ~40km and ~80km. Then turns to the equator at ~50km. We find that the background wind in Figure 5j is weaker than that in Figure 5i, but the instability is stronger. This finding indicates that E2 has absorbed sufficient energy to be amplified under the background conditions during days 219-224 (Figure 5j).

Figures 6a and 6b show that the E3 planetary waves have wave periods of ~29 h on days 151-154 and 201-204. The temperature spatial structure of E3 events presents a dual structure, as shown in Figures 6c and 6d. The maximum temperature amplitude of E3 is ~7K (~50km) on days

https://doi.org/10.5194/acp-2021-461
Preprint. Discussion started: 17 June 2021
© Author(s) 2021. CC BY 4.0 License.


151-154, and the other peak is ~5K (~60km). The temperature amplitude of E3 is ~5K (~50, ~60km) on days 201-204. The spatial structures of zonal wind and meridional wind of E3 are shown in Figures 6e, 6f, 6g, and 6h. The maximum amplitudes of zonal and meridional winds occur at ~50˚S and ~60km, and ~60˚S and ~60km. The maximum zonal wind is ~10 m/s, while the meridional wind is slightly stronger than the zonal wind at ~15 m/s. The EP flux of E3 is similar to that of E2. We find that instability at mid-high latitudes between ~50 and ~70km dramatically amplifies the E3 propagation and that the interaction near the critical layer enhances the process (Figures 6i and 6j). It is worth noting that the region of background wind at ~50-60˚S and ~60-70km is similar during days 151-154 and 201-204, while the former is strong instability and the latter is weak instability. This finding indicates that the strong instability provides sufficient energy for the amplification for E3 propagation on days 151-154.

The wave period of E4 reaches ~25 h and ~21h during days 127-130 and 213-216 in Figures 7a and 7b. The maximum temperature amplitude of E4 occurs on days 127-130, reaching ~4K (~50km), the other peak is ~3K (~60km). The temperature amplitude is ~3K (~50, ~60 km) on days 213-216, as displayed in Figure 7d. The spatial structures of zonal wind and meridional wind of E4 are shown in Figures 7e, 7f, 7g, and 7h. The maximum amplitudes of zonal and meridional winds occur at ~50˚S and ~60km, and ~60˚S and ~60km. The maximum zonal wind is ~8 m/s, while

https://doi.org/10.5194/acp-2021-461
Preprint. Discussion started: 17 June 2021
© Author(s) 2021. CC BY 4.0 License.



the meridional wind is slightly stronger than the zonal wind at ~10 m/s. We find that the instability in the mid-high latitudes between ~50 and ~70km and the interaction near the critical layer greatly enhance the propagation and amplification of E4 EP flux, as shown in Figures 7i and 7j. The weak background wind and strong instability appear on days 127-130, while the strong background wind and weak instability appear on days 213-216. This finding indicates that E4 is difficult to obtain sufficient energy to be amplified under background conditions during days 213-216. The amplitude on 127-130 days is stronger.

### 3.2 In the Northern Hemisphere

Figure 8 shows that the E1 and E2 (E3) are distributed at ~70-80˚N, and ~60-70˚N at ~59.2km, respectively. E1 events occur on days 25-34, 41-50, and 339-348 respectively, in which the maximum temperature amplitude of days 41-50 reaches ~8K, as shown in Figure 8a. In addition, the wave periods of E1 decreased from a maximum of ~118 h (days 25-34) to ~80 h (days 41-50), indicating that the wave period of E1 is unstable in the NH. Clearly, the E2 events occur on days 25-30, 69-74, 317-322, and 341-346, of which the corresponding wave periods are ~36, ~53, ~52, and ~48 h, and the maximum temperature amplitude reaches ~7K on days 69-74, as shown in Figure 8b. Figure 8c shows two E3 events. The strongest temperature amplitude of E3 occurs on days 35-38 and reaches ~3K, and the other one occurs on days 53-56. The wave period of E3 is relatively

https://doi.org/10.5194/acp-2021-461
Preprint. Discussion started: 17 June 2021
© Author(s) 2021. CC BY 4.0 License.

Atmospheric Chemistry and Physics Discussions
Open Access
EGU

stable at ~29 h and ~27 h. We did not study the E4 event in the NH, because E4 is weak.

The spectra, spatial structures of temperature, zonal and meridional wind, and diagnostic analysis of E1 are extracted from the corresponding representative events, as shown in Figure 9. From Figures 9a and 9b, the wave periods of planetary E1 waves on days 25-34 and 41-50 are ~118 h and ~80 h, respectively. The temperature spatial structure of the E1 event presents an obvious dual amplitude structure (~60km, ~70km). From Figure 9d, the strongest temperature amplitude of E1 appears at ~60km on days 41-50, with an amplitude of ~10K, and the rest peak is ~8K (~70km). The temperature amplitude of ~7K appears on days 25-34, and the rest is ~4K (~70km), as shown in Figure 9c. The spatial structures of zonal wind and meridional wind of E1 are shown in Figures 9e, 9f, 9g, and 9h. The maximum amplitudes of zonal and meridional winds occur at ~50˚N and ~70km, and ~80˚N and ~70km. The maximum zonal wind is ~14 m/s, while the meridional wind is slightly stronger than the zonal wind at ~18 m/s. The results show that E1 is more conducive to the propagation in winter in the NH, and the instability at mid-latitude between ~60 and ~80 km and the interaction near the critical layer dramatically amplify the propagation of E1, which eventually turns toward the equator in the Arctic (Figures 9i and 9j). Obviously, the instability on days 25-34 and 41-50 is relatively weak, but the former has stronger background winds. This

https://doi.org/10.5194/acp-2021-461
Preprint. Discussion started: 17 June 2021
© Author(s) 2021. CC BY 4.0 License.
Atmospheric Chemistry and Physics Discussions

finding indicates that the background condition on days 41-50 is conducive to the propagation and amplification for E1.

From Figures 10a and 10b, the wave period of E2 on days 25-30 and 69-74 reaches ~36h and ~53h. The maximum temperature amplitude of E2 appears on days 69-74, reaches ~10K (~60km), and the other peak is ~7K (~70km). The maximum temperature amplitude is ~5K (~60km) during days 25-30, and another peak is ~4K (~70km). The spatial structures of zonal wind and meridional wind of E2 are shown in Figures 10e, 10f, 10g, and 10h. The maximum amplitudes of zonal and meridional winds occur at ~50˚N and ~70km, and ~60˚N and ~70km. The maximum zonal and meridional winds are ~7 (~18) m/s on days 35-30 (69-74). Clearly, the instability at a mid-high latitude between ~40 and ~80 km and the interaction near the critical layer dramatically amplify the propagation of E2, which eventually turns toward the equator, as displayed in Figures 10i and 10j. Obviously, the temperature amplitude is stronger on days 69-74, which indicates that E2 obtains sufficient energy for amplification under the background condition.

The E3 planetary waves have wave periods of ~29h and ~27h on days 35-38 and 53-56, as shown in Figures 11a, and 11b. Clearly, from Figures 11c, and 11d, the maximum temperature amplitude of E3 is ~6K (~70km) on days 35-38, and another peak is ~5K (~60km). The peak temperature amplitude is ~4K (~60, ~70 km) on days 53-56. The spatial structures of

https://doi.org/10.5194/acp-2021-461
Preprint. Discussion started: 17 June 2021
© Author(s) 2021. CC BY 4.0 License.



zonal wind and meridional wind of E3 are shown in Figures 11e, 11f, 11g, and 11h. The maximum amplitudes of zonal and meridional winds occur at ~40˚N and ~70km, and ~50˚N and ~70km. The maximum zonal and meridional winds are ~15 (~7) and ~22 (~13) m/s on days 35-38 (53-56). Obviously, the instability at mid-latitude between ~60 and ~70 km and the interaction near the critical layer dramatically amplify the propagation of E3, as shown in Figures 11i and 11j. The background wind is similar on days 35-38 and 53-56, and the former is more unstable. This finding indicates that the E3 in propagation is more likely to get sufficient energy to be amplified on days 35-38.

### 3.3 Comparison between SH and NH

We find that the observed latitude and maximum amplitude for eastward planetary waves (E1, E2, E3, E4) decrease and weaken with increasing zonal wavenumber in the SH, reaching ~70-80˚S, ~60-70˚S, ~60-70˚S, and ~50-60˚S, and ~10K, ~9K, ~6K, and ~3K, respectively. In addition, the occurrence date is earlier with increasing zonal wavenumber. The temperature spatial structure shows a dual-peak structure (~50 and ~60km), primarily located at ~50km. The maximum zonal wind amplitudes of E1 and E2, E3 and E4 are almost the equivalents, which are ~20 m/s and ~10 m/s respectively. The maximum meridional wind amplitude of E1, E2, E3 and E4 are ~17 m/s, ~27 m/s, ~16 m/s, and ~11 m/s respectively. The wave period of E1 tends to get shorter from 5 to 3 days, while E2 and E3

https://doi.org/10.5194/acp-2021-461
Preprint. Discussion started: 17 June 2021
© Author(s) 2021. CC BY 4.0 License.


are close to ~40 h and ~30 h, while E4 remains at ~24 h. E1, E2, E3, and E4 are more favorable to propagation in the SH winter and are dramatically amplified by the mean flow instabilities at middle latitudes between ~40 and ~70 km. In addition, E1 upward propagating EP flux may be influenced by the instability and background wind at the Antarctic ~50km.

The observed latitudes of E1, E2 (E3) decrease with increasing wavenumber in the NH, which are ~70-80˚N, ~60-70˚N, and ~60-70˚N. The temperature spatial structure of E1, E2, and E3 presents a dual-peak structure, primarily located at ~70km, reaches ~10K, ~9K, and ~6K. The maximum zonal wind amplitude appears at ~50-80˚N and ~60km. E1, E2, E3, and E4 are almost the equivalent, which is ~18 m/s respectively. The maximum meridional wind amplitude appears at ~50-80˚N and ~60km. The maximum amplitudes of E1, E2, and E3 are ~22 m/s, ~18 m/s, and ~22 m/s respectively. The wave period of E1 tends to be shorter from 5-3 days, and E2 and E3 are close to ~48 h and ~30 h. In addition, E1, E2, and E3 are more favorable to propagation in the NH winter and are dramatically amplified by the mean flow instabilities at middle latitudes between ~40 and ~70 km.

## 4 Summary and Conclusions

We present for the first time an extensive study of the global variation for eastward planetary wave activity, including zonal wave numbers of -1 (E1), -2 (E2), -3 (E3), -4 (E4), in the stratosphere and mesosphere using

https://doi.org/10.5194/acp-2021-461
Preprint. Discussion started: 17 June 2021
© Author(s) 2021. CC BY 4.0 License.


the MERRA-2 temperature and wind observations in 2019. The temperature and wind amplitudes and wave periods of each event were determined by 2-D least-squares fitting. Our study includes the spatial and temporal behaviors of the eastward planetary waves in both hemispheres with a comprehensive diagnostic analysis on their propagation and amplification. The key findings of the study are summarized as follows:

1. The latitudes for the maximum (temperature, zonal and meridional wind) amplitudes of E1, E2, E3, and E4 decrease with increasing wavenumber in the SH and NH. The E1, E2, E3, and E4 events occur earlier with increasing zonal wavenumber in the SH. In addition, eastward wave modes exist during summer periods with westward background wind in both hemispheres.
2. The temperature spatial structures of E1, E2, E3, and E4 present a double-peak structure, which is located at ~50km and ~60km in SH, ~60km, and ~70km in SH. In addition, the lower peak is usually larger than the higher one.
3. The maximum (temperature, zonal and meridional wind) amplitudes of E1, E2, and E3 decrease with increasing zonal wavenumber in the SH and NH. The maximum temperature amplitudes in the SH are slightly larger and lie lower than those in the NH. In addition, the meridional wind amplitudes are slightly larger than the zonal wind in the SH and NH.
4. The period of the E1 mode varies from 3 to 5 days in both hemispheres,

https://doi.org/10.5194/acp-2021-461
Preprint. Discussion started: 17 June 2021
© Author(s) 2021. CC BY 4.0 License.



while the period of E2 mode is slightly longer in the NH (48 h) than in the SH (40 h). The periods of E3 are ~30 h in both SH and NH, and the period of E4 is ~24 h.

5. The eastward planetary wave is more favorable to propagate in the winter hemisphere and is dramatically amplified by the mean flow instabilities and appropriate background winds at polar and middle latitudes between ~40 and ~80 km. Furthermore, the amplification of planetary waves through wave-mean flow interaction most easily occurs near its critical layer. In addition, the direction of EP flux ultimately points towards the equator.

6. The strong instability and appropriate background wind in the lower layer of the Antarctic region may provide sufficient energy to promote the E1 propagation and amplification to the upper layer.

This study demonstrates how the background zonal wind in the polar middle atmosphere affects the dynamics of eastward planetary waves in the polar middle atmosphere.

https://doi.org/10.5194/acp-2021-461
Preprint. Discussion started: 17 June 2021
© Author(s) 2021. CC BY 4.0 License.



*Data availability.* MERRA-2 data are available at http://disc.gsfc.nasa.gov.

*Author contributions.* LT carried out the data processing and analysis and wrote the manuscript. SYG and XKD contributed to reviewing the article.

*Competing interests.* The authors declare that they have no conflict of interest.

*Acknowledgements.* This work was performed in the framework of the Space Physics Research (SPR). The authors thank NASA for free online access to the MERRA-2 temperature reanalysis.

*Acknowledgments.* This research work was supported by the National Natural Science Foundation of China (41704153, 41874181, and 41831071).

https://doi.org/10.5194/acp-2021-461
Preprint. Discussion started: 17 June 2021
© Author(s) 2021. CC BY 4.0 License.

Atmospheric Chemistry and Physics
Discussions

# References

Alexander, S. P. and Shepherd, M. G.: Planetary wave activity in the polar lower stratosphere, ATMOSPHERIC CHEMISTRY AND PHYSICS, 10, 707-718, 2010.

Andrews, D., Leovy, C., and Holton, J.: Volume 40. Middle Atmosphere Dynamics, 1987.

Bali, K., Dey, S., Ganguly, D., and Smith, K. R.: Space-time variability of ambient PM2.5 diurnal pattern over India from 18-years (2000–2017) of MERRA-2 reanalysis data, Atmos. Chem. Phys. Discuss., 2019, 1-23, 10.5194/acp-2019-731, 2019.

Coy, L., Štajner, I., DaSilva, A. M., Joiner, J., Rood, R. B., Pawson, S., and Lin, S. J.: High-Frequency Planetary Waves in the Polar Middle Atmosphere as Seen in a Data Assimilation System, Journal of the Atmospheric Sciences, 60, 2975-2992, 10.1175/1520-0469(2003)060<2975:Hpwitp>2.0.Co;2, 2003.

Gu, S. Y., Liu, H. L., Dou, X., and Jia, M.: Ionospheric Variability Due to Tides and Quasi-Two Day Wave Interactions, Journal of Geophysical Research: Space Physics, 2018a.

Gu, S. Y., Liu, H. L., Dou, X., and Li, T.: Influence of the sudden stratospheric warming on quasi-2-day waves, Atmospheric Chemistry and Physics, 16, 1-45, 2016a.

Gu, S. Y., Liu, H. L., Pedatella, N. M., Dou, X., and Liu, Y.: On the wave number 2 eastward propagating quasi 2day wave at middle and high latitudes, Journal of Geophysical Research: Space Physics, 2017.

Gu, S. Y., Liu, H. L., Pedatella, N. M., Dou, X., and Shu, Z.: The quasi-2 day wave activities during 2007 boreal summer period as revealed by Whole Atmosphere Community Climate Model, Journal of Geophysical Research: Space Physics, 2016b.

Gu, S. Y., Ruan, H., Yang, C. Y., Gan, Q., and Wang, N.: The Morphology of the 6-Day Wave in Both

https://doi.org/10.5194/acp-2021-461
Preprint. Discussion started: 17 June 2021
© Author(s) 2021. CC BY 4.0 License.



the Neutral Atmosphere and F Region Ionosphere Under Solar Minimum Conditions, Journal of Geophysical Research: Space Physics, 123, 2018b.

Gu, S. Y., Xiankang, D., Dora, P., Wen, Y., and Tingdi, C.: Investigation of the Abnormal Quasi 2-Day Wave Activities During the Sudden Stratospheric Warming Period of January 2006, Journal of Geophysical Research: Space Physics, 123, 2018c.

Gu, S. Y., Li, T., Dou, X., Wu, Q., Mlynczak, M. G., and Russell, J. M.: Observations of Quasi-Two-Day wave by TIMED/SABER and TIMED/TIDI, Journal of Geophysical Research Atmospheres, 118, 1624–1639, 2013.

Gu, S. Y., Dou, X. K., Yang, C. Y., Jia, M. J., Huang, K. M., Huang, C. M., and Zhang, S. D.: Climatology and Anomaly of the Quasi-Two Day Wave Behaviors during 2003-2018 Austral Summer Periods, Journal of Geophysical Research Space Physics, 2018d.

Lainer, M., Hocke, K., and Kämpfer, N.: Long-term observation of mid-latitude quasi 2-day waves by a water vapor radiometer, Atmospheric Chemistry & Physics, 1-22, 2018.

Li, H., Kedzierski, R. P., and Matthes, K.: On the forcings of the unusual Quasi-Biennial Oscillation structure in February 2016, Atmospheric Chemistry and Physics, 20, 6541-6561, 2020.

Lilienthal, F. and Jacobi, C.: Meteor radar quasi 2-day wave observations over 10 years at Collm (51.3° N, 13.0° E), ATMOSPHERIC CHEMISTRY AND PHYSICS, 15, 2015.

Limpasuvan, V. and Wu, D. L.: Anomalous two-day wave behavior during the 2006 austral summer, Geophysical Research Letters, 36, L04807, 2009.

Liu and H.-L.: The 6.5-day wave and its seasonal variability in the middle and upper atmosphere, Journal of Geophysical Research Atmospheres, 109, -, 2004.

Liu, G., England, S. L., and Janches, D.: Quasi Two-, Three-, and Six-Day Planetary-Scale Wave

https://doi.org/10.5194/acp-2021-461
Preprint. Discussion started: 17 June 2021
© Author(s) 2021. CC BY 4.0 License.
Atmospheric Chemistry and Physics
Open Access
EGU
Discussions

Oscillations in the Upper Atmosphere Observed by TIMED/SABER Over ~17 Years During 2002–2018, Journal of Geophysical Research: Space Physics, 124, 2019.

Lu, X., Chu, X., Fuller-Rowell, T., Chang, L., Fong, W., and Yu, Z.: Eastward propagating planetary waves with periods of 1–5 days in the winter Antarctic stratosphere as revealed by MERRA and lidar, Journal of Geophysical Research: Atmospheres, 118, 9565-9578, https://doi.org/10.1002/jgrd.50717, 2013.

Manney, G., L., Randel, W., and J.: Instability at the Winter Stratopause: A Mechanism for the 4-Day Wave, J.atmos.sci, 1993.

Matthias, V. and Ern, M.: On the origin of the mesospheric quasi-stationary planetary waves in the unusual Arctic winter 2015/2016, Atmospheric Chemistry and Physics, 18, 4803-4815, 2018.

Meek, C. E., Manson, A. H., Franke, S. J., Singer, W., Hoffmann, P., Clark, R. R., Tsuda, T., Nakamura, T., Tsutsumi, M., and Hagan, M.: Global study of northern hemisphere quasi-2-day wave events in recent summers near 90 km altitude, Journal of Atmospheric and Solar-Terrestrial Physics, 58, 1401-1411, 1996.

Merzlyakov, E. G. and Pancheva, D. V.: The 1.5–5-day eastward waves in the upper stratosphere–mesosphere as observed by the Esrange meteor radar and the SABER instrument, Journal of Atmospheric and Solar-Terrestrial Physics, 69, 2102-2117, 2007.

Molod, A., Takacs, L., Suarez, M., and Bacmeister, J.: Development of the GEOS-5 atmospheric general circulation model: evolution from MERRA to MERRA2, Geoscientific Model Development,8,5(2015-05-12), 7, 1339-1356, 2015.

Molod, A., Takacs, L., Suarez, M., Bacmeister, J., Song, I. S., and Eichmann, A.: The GEOS-5 Atmospheric General Circulation Model: Mean Climate and Development from MERRA to

https://doi.org/10.5194/acp-2021-461
Preprint. Discussion started: 17 June 2021
© Author(s) 2021. CC BY 4.0 License.


Fortuna, 2012.

Palo, S. E., Roble, R. G., and Hagan, M. E.: Middle atmosphere effects of the quasi-two-day wave determined from a General Circulation Model, Earth Planets & Space, 51, 629-647, 1999.

Palo, S. E., Forbes, J. M., Zhang, X., Russell, J. M., and Mlynczak, M. G.: An eastward propagating two-day wave: Evidence for nonlinear planetary wave and tidal coupling in the mesosphere and lower thermosphere, Geophysical Research Letters, 340, 248-265, 2007.

Pancheva, D., Mukhtarov, P., and Siskind, D. E.: Climatology of the quasi-2-day waves observed in the MLS/Aura measurements (2005–2014), Journal of Atmospheric and Solar-Terrestrial Physics, 171, 2017.

Rao, N. V., Ratnam, M. V., Vedavathi, C., Tsuda, T., Murthy, B. V. K., Sathishkumar, S., Gurubaran, S., Kumar, K. K., Subrahmanyam, K. V., and Rao, S. V. B.: Seasonal, inter-annual and solar cycle variability of the quasi two day wave in the low-latitude mesosphere and lower thermosphere, Journal of Atmospheric & Solar Terrestrial Physics, S1364682616304084, 2016.

Salby, M. L.: The 2-day wave in the middle atmosphere: Observations and theory, Journal of Geophysical Research Atmospheres, 86, 9654-9660, 1981.

Sandford, D. J., Schwartz, M. J., and Mitchell, N. J.: The wintertime two-day wave in the Polar Stratosphere, Mesosphere and lower Thermosphere, Atmospheric Chemistry & Physics Discussions, 7, 749-755, 2007.

Stray, N. H., Orsolini, Y. J., Espy, P. J., Limpasuvan, V., and Hibbins, R. E.: Observations of planetary waves in the mesosphere-lower thermosphere during stratospheric warming events, Atmospheric Chemistry and Physics, 15, 4997-5005, 2015.

Sun, J., Veefkind, J. P., van Velthoven, P., Tilstra, L. G., Chimot, J., Nanda, S., and Levelt, P. F.: Defining

https://doi.org/10.5194/acp-2021-461
Preprint. Discussion started: 17 June 2021
© Author(s) 2021. CC BY 4.0 License.

aerosol layer height for UVAI interpretation using aerosol vertical distributions characterized by MERRA-2, Atmos. Chem. Phys. Discuss., 2020, 1-36, 10.5194/acp-2020-39, 2020.

Tunbridge, V. M., Sandford, D. J., and Mitchell, N. J.: Zonal wave numbers of the summertime 2 day planetary wave observed in the mesosphere by EOS Aura Microwave Limb Sounder, Journal of Geophysical Research Atmospheres, 116, -, 2011.

Ukhov, A., Mostamandi, S., da Silva, A., Flemming, J., Alshehri, Y., Shevchenko, I., and Stenchikov, G.: Assessment of natural and anthropogenic aerosol air pollution in the Middle East using MERRA-2, CAMS data assimilation products, and high-resolution WRF-Chem model simulations, Atmos. Chem. Phys., 20, 9281-9310, 10.5194/acp-20-9281-2020, 2020.

Venne, D. E. and Stanford, J. L.: Observation of a 4–Day Temperature Wave in the Polar Winter Stratosphere, J.atmos, 36, 2016-2019, 2010.

Wang, J. C., Chang, L. C., Yue, J., Wang, W., and Siskind, D. E.: The quasi 2day wave response in TIME-GCM nudged with NOGAPS-ALPHA, Journal of Geophysical Research Space Physics, 2017.

Wu, W. S., Purser, R. J., and Parrish, D. F.: Three-Dimensional Variational Analysis with Spatially Inhomogeneous Covariances, Monthly Weather Review, 130, 2905, 2002.

Xiong, J., Wan, W., Ding, F., Liu, L., Hu, L., and Yan, C.: Two Day Wave Traveling Westward With Wave Number 1 During the Sudden Stratospheric Warming in January 2017, Journal of Geophysical Research: Space Physics, 2018.

Yadav, S., Vineeth, C., Kumar, K. K., Choudhary, R. K., and Centre, V. S. S.: Role of the phase of Quasi-Biennial Oscillation in modulating the influence of SSW on Equatorial Ionosphere, 2019 URSI Asia-Pacific Radio Science Conference (AP-RASC), Yamazaki, K., Nakamura, T., Ukita, J., and Hoshi, K.: A tropospheric pathway of the stratospheric quasi-biennial oscillation (QBO) impact on the boreal winter polar vortex, 10.5194/acp-2019-1119, 2020.

https://doi.org/10.5194/acp-2021-461
Preprint. Discussion started: 17 June 2021
© Author(s) 2021. CC BY 4.0 License.



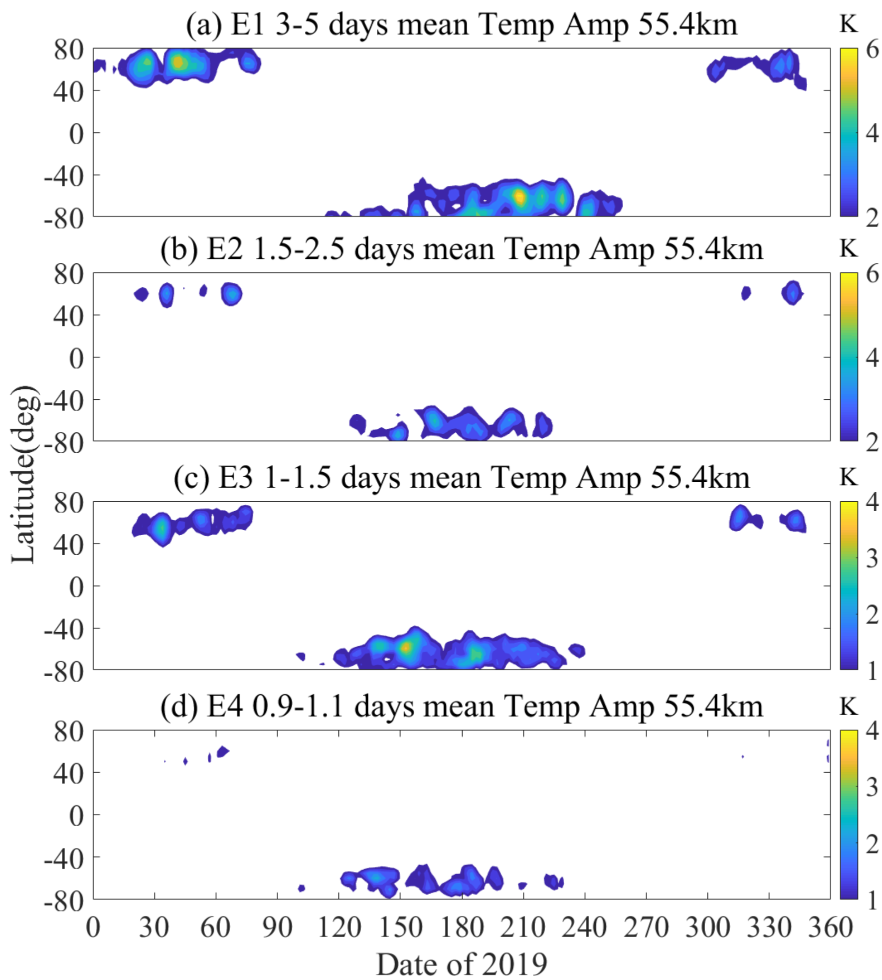


591

592 **Figure 1.** The global latitude-temporal variation structures of the (a) E1, (b) E2, (c) E3,

593 (d) E4 planetary waves during 2019.

https://doi.org/10.5194/acp-2021-461
Preprint. Discussion started: 17 June 2021
© Author(s) 2021. CC BY 4.0 License.



594 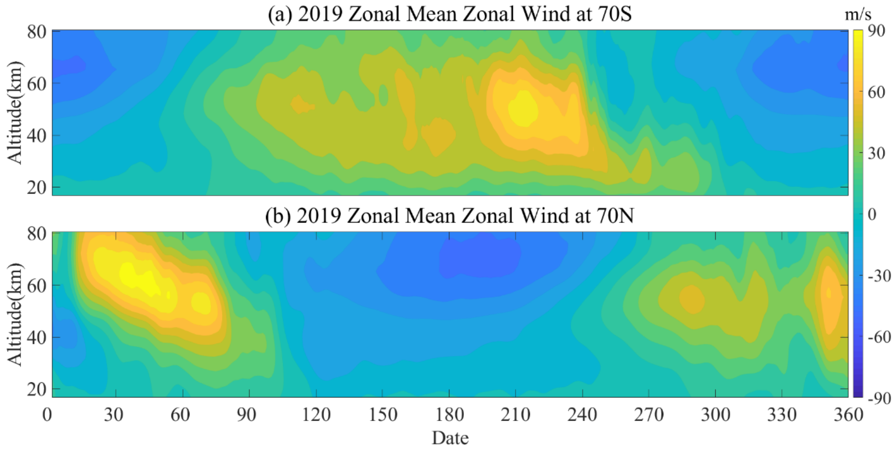


595 **Figure 2.** The zonal mean zonal wind variations of the (a) the 70S and (b) 70N during

596 2019.

https://doi.org/10.5194/acp-2021-461
Preprint. Discussion started: 17 June 2021
© Author(s) 2021. CC BY 4.0 License.

Atmospheric Chemistry and Physics Discussions

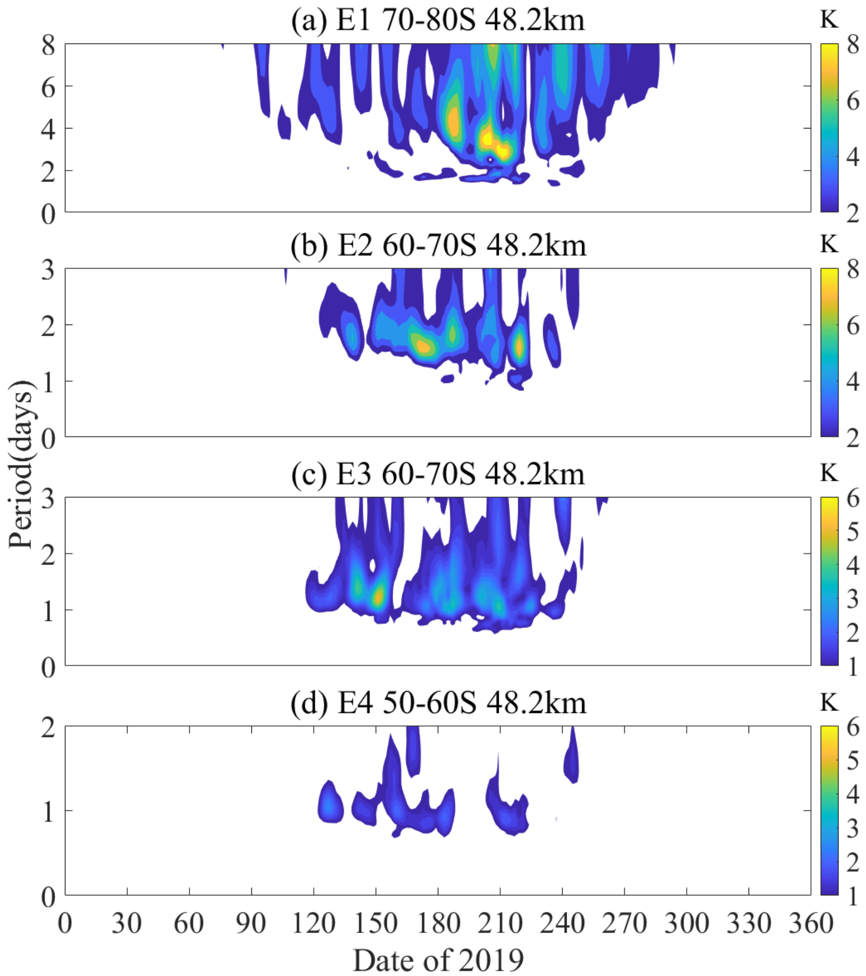


**Figure 3.** The temporal variations of the (a) E1, (b) E2, (c) E3, (d) E4 QTDWs during 2019 austral winter period.

https://doi.org/10.5194/acp-2021-461
Preprint. Discussion started: 17 June 2021
© Author(s) 2021. CC BY 4.0 License.

Atmospheric Chemistry and Physics
Discussions

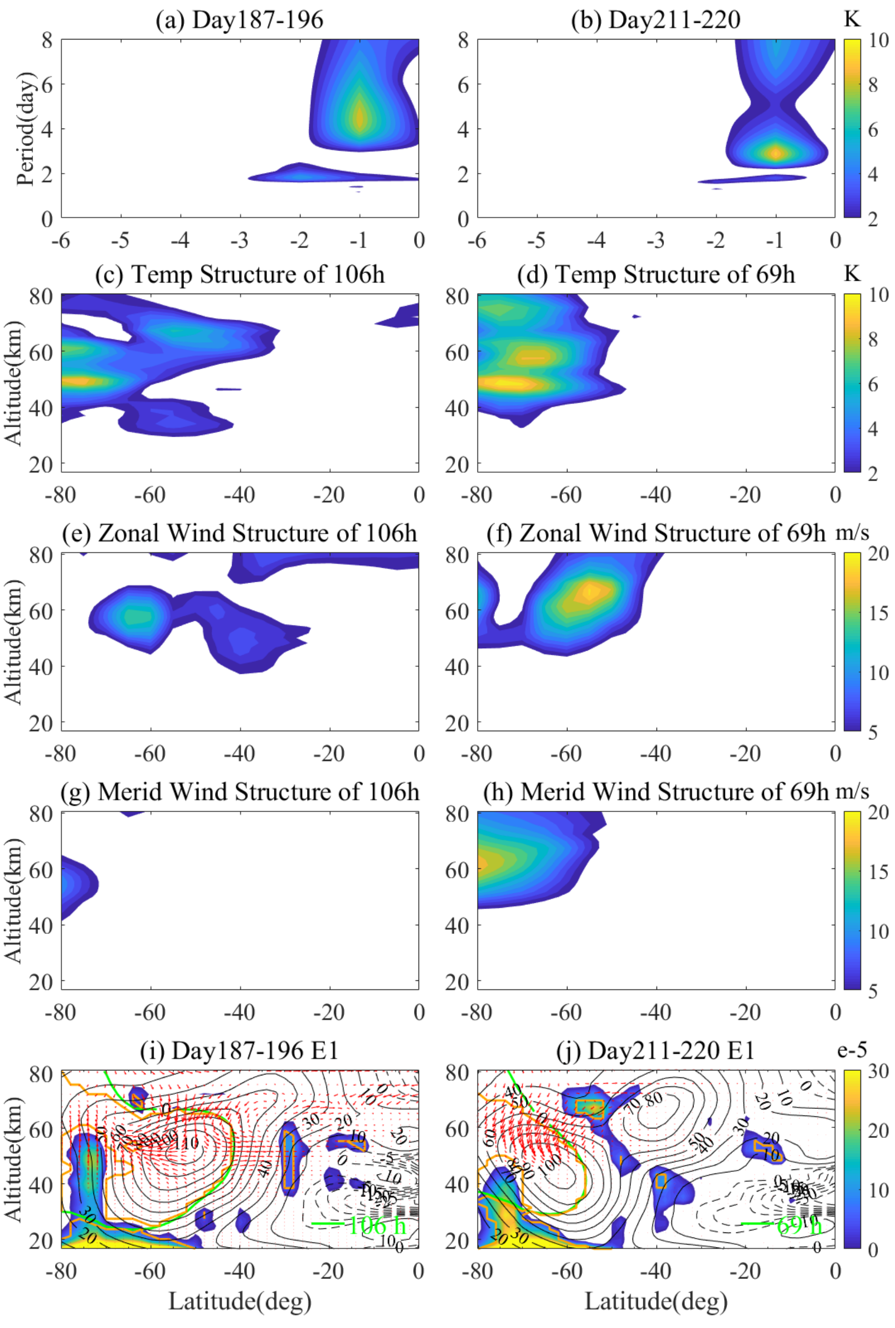


600

601 **Figure 4.** The (a, b) spectra, (c, d) temperature spatial structures, (e, f) zonal wind

602 spatial structures, (g, h) meridional wind spatial structures, and (i, j) diagnostic analysis

https://doi.org/10.5194/acp-2021-461
Preprint. Discussion started: 17 June 2021
© Author(s) 2021. CC BY 4.0 License.
Atmospheric Chemistry and Physics Discussions
Open Access

of the E1 typical events during 2019 austral winter period. The MERRA-2 temperature data observations at 48.2km and 70-80˚S during days 187–196 (Figure 4a), 211–220 (Figure 4d) are utilized, respectively. The instability (blue shaded region), EP fluxes (red arrow), and critical layers (green line) for E1 typical event. The green line represents critical layers of the E1 with the natural period. Regions enclosed by orange solid lines are characterized by the positive refractive index for the E1.

https://doi.org/10.5194/acp-2021-461
Preprint. Discussion started: 17 June 2021
© Author(s) 2021. CC BY 4.0 License.



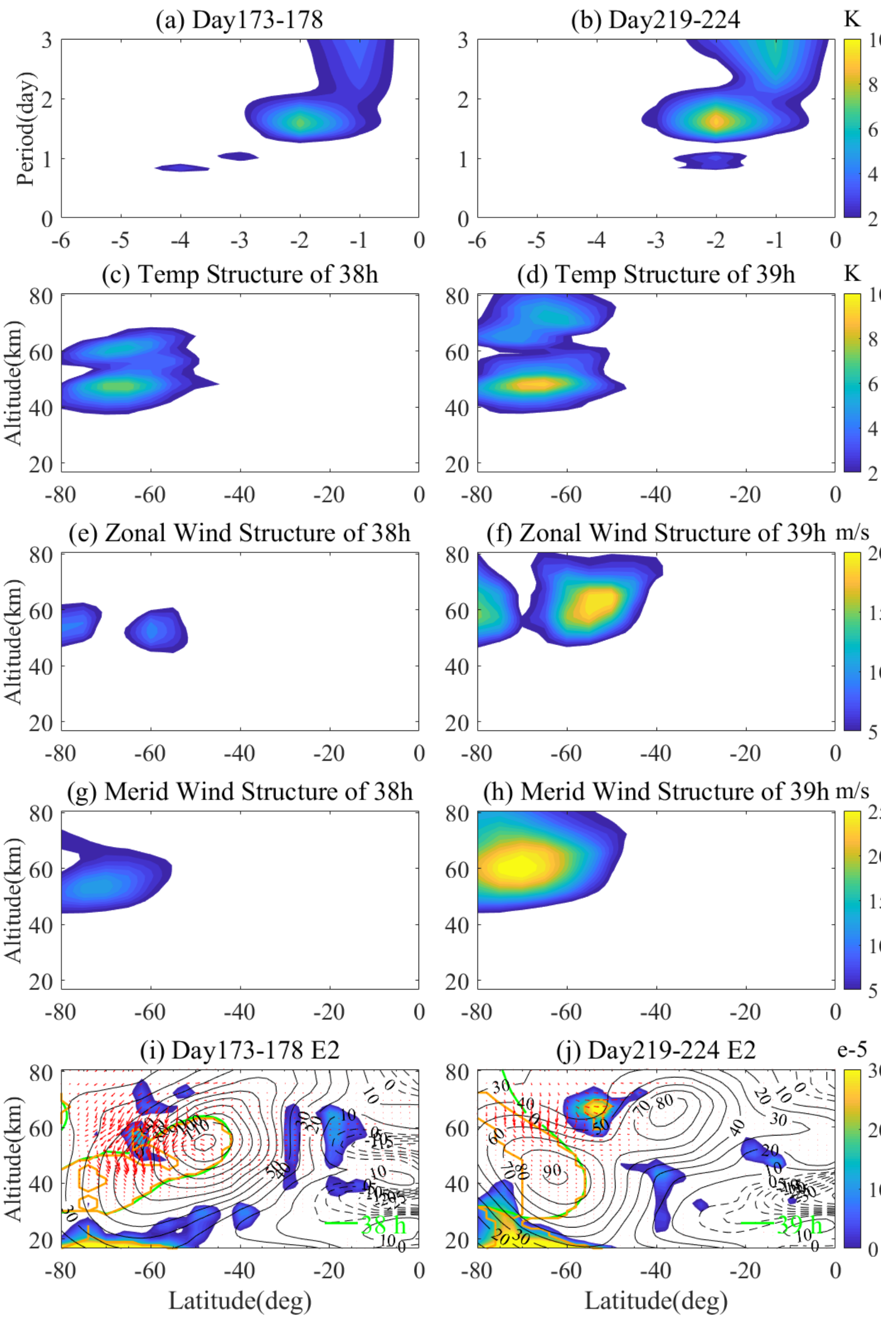


**Figure 5.** The same as Figure 4 but for the E2 during the 2019 austral winter period.

https://doi.org/10.5194/acp-2021-461
Preprint. Discussion started: 17 June 2021
© Author(s) 2021. CC BY 4.0 License.
Atmospheric Chemistry and Physics
Discussions

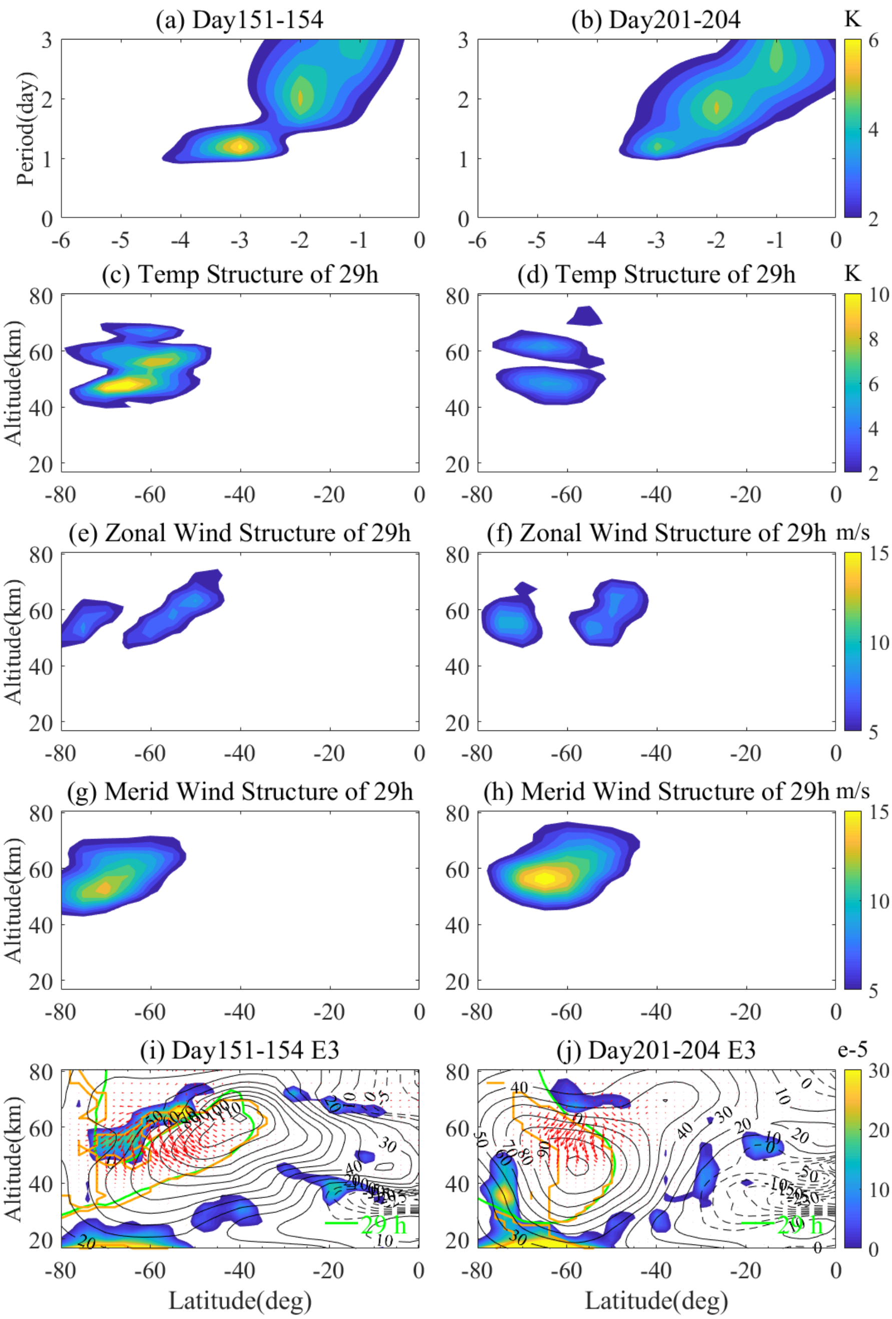


612 **Figure 6.** The same as Figure 4 but for the E3 during the 2019 austral winter period.

https://doi.org/10.5194/acp-2021-461
Preprint. Discussion started: 17 June 2021
© Author(s) 2021. CC BY 4.0 License.

Atmospheric Chemistry and Physics
Discussions

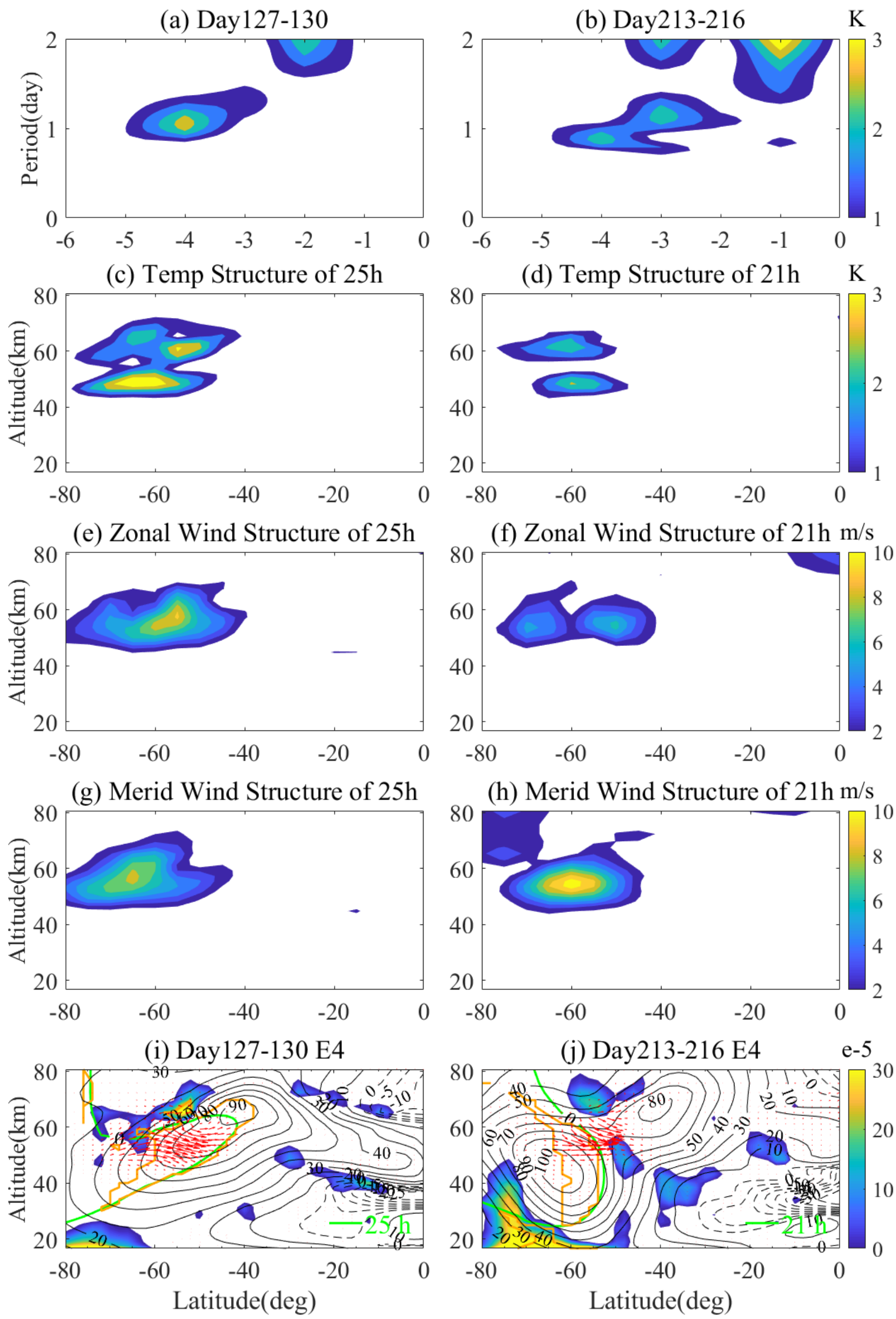


613

614 **Figure 7.** The same as Figure 4 but for the E4 during the 2019 austral winter period.

https://doi.org/10.5194/acp-2021-461
Preprint. Discussion started: 17 June 2021
© Author(s) 2021. CC BY 4.0 License.
Atmospheric Chemistry and Physics
Discussions

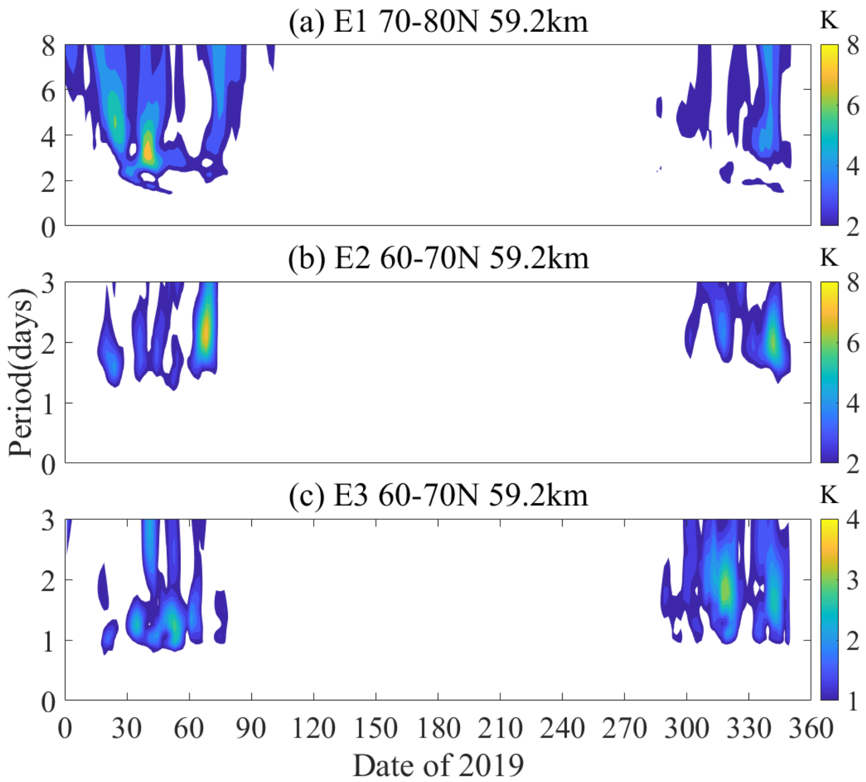


**Figure 8.** The temporal variations of the (a) E1, (b) E2, and (c) E3 QTDWs during the 2019 boreal winter period.

https://doi.org/10.5194/acp-2021-461
Preprint. Discussion started: 17 June 2021
© Author(s) 2021. CC BY 4.0 License.

Atmospheric Chemistry and Physics
Discussions

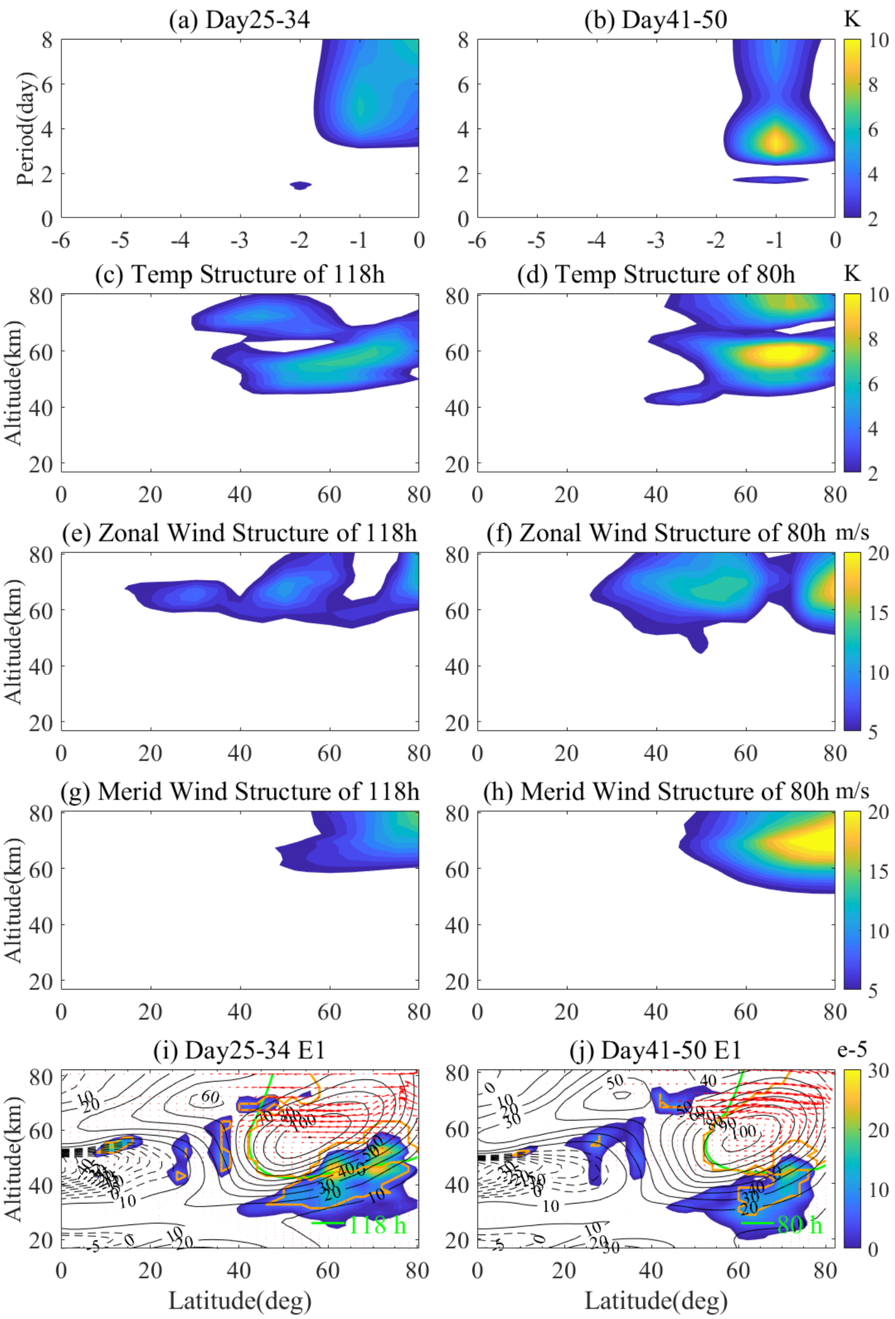


618

619 **Figure 9.** he (a, b) spectra, (c, d) temperature spatial structures, (e, f) zonal wind spatial

620 structures, (g, h) meridional wind spatial structures, and (i, j) diagnostic analysis of the

https://doi.org/10.5194/acp-2021-461
Preprint. Discussion started: 17 June 2021
© Author(s) 2021. CC BY 4.0 License.

621 E1 typical events during 2019 boreal winter period. The E1 events at 48.2km and 70-

622 80°N were obtained from the MERRA-2 reanalysis.

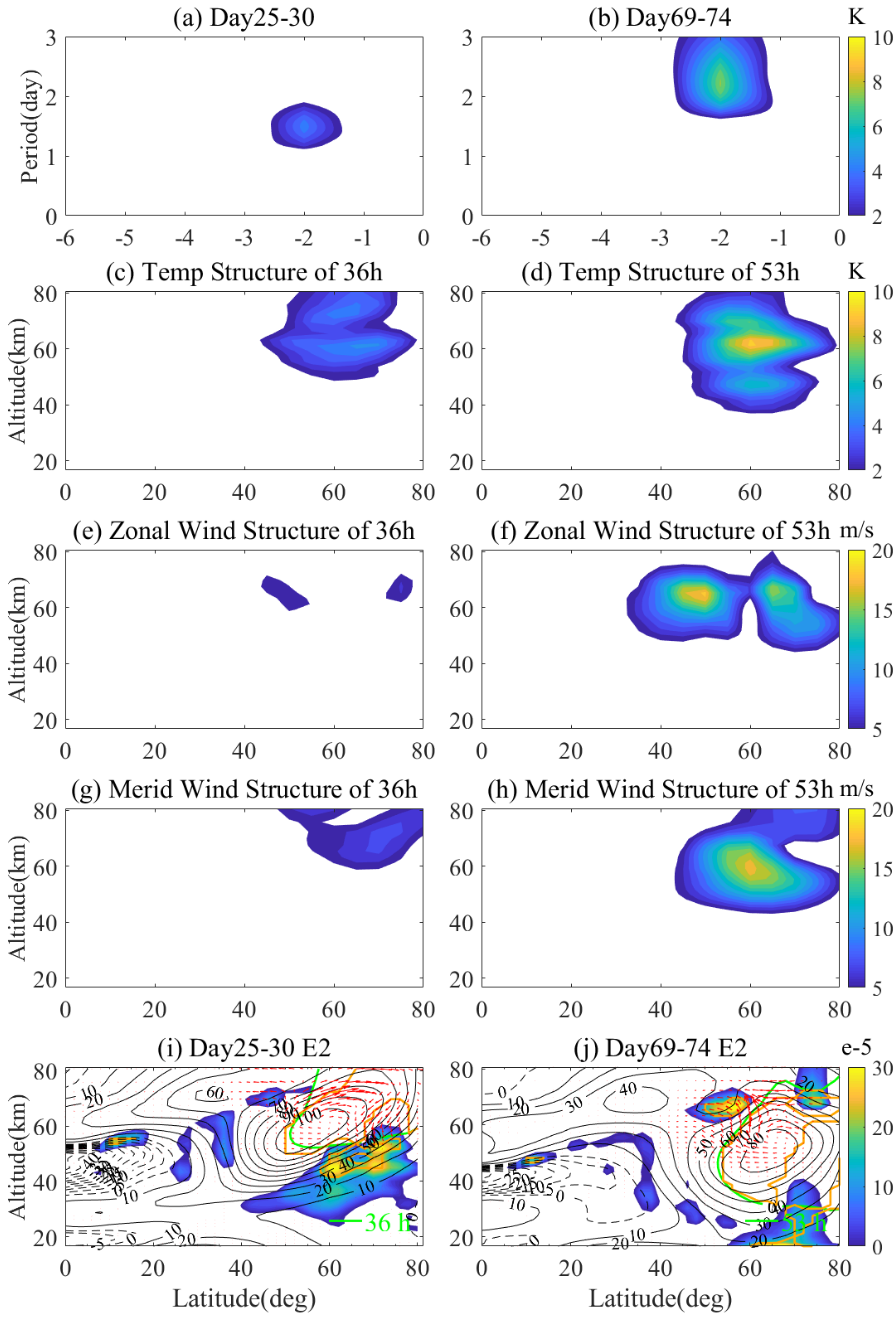


623

https://doi.org/10.5194/acp-2021-461
Preprint. Discussion started: 17 June 2021
© Author(s) 2021. CC BY 4.0 License.


**Figure 10.** The same as Figure 9 but for the E2 during the 2019 boreal winter period.

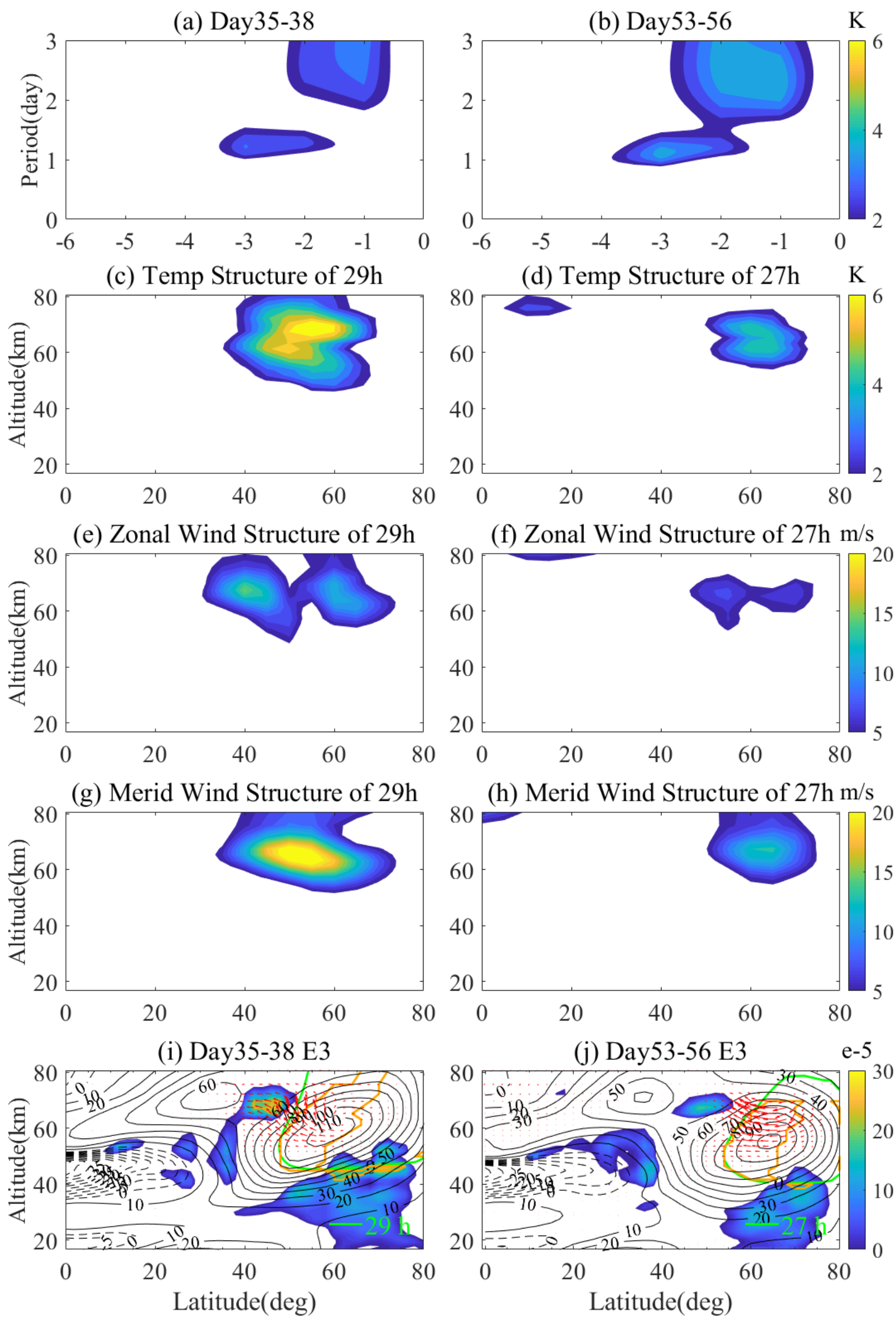


**Figure 11.** The same as Figure 9 but for the E3 during the 2019 boreal winter period.